



REVIEW

# Recent advances in diffusion neuroimaging: applications in the developing preterm brain [version 1; referees: 2 approved]

Diliana Pecheva<sup>1</sup>, Christopher Kelly<sup>1</sup>, Jessica Kimpton<sup>1</sup>, Alexandra Bonthron<sup>1</sup>, Dafnis Batalle <sup>1</sup>, Hui Zhang<sup>2</sup>, Serena J. Counsell <sup>1</sup>

<sup>1</sup>Centre for the Developing Brain, School of Biomedical Engineering & Imaging Sciences, King's College London, London, UK

<sup>2</sup>Department of Computer Science & Centre for Medical Image Computing, University College London, London, UK

**v1** **First published:** 21 Aug 2018, 7(F1000 Faculty Rev):1326 (doi: 10.12688/f1000research.15073.1)  
**Latest published:** 21 Aug 2018, 7(F1000 Faculty Rev):1326 (doi: 10.12688/f1000research.15073.1)

**Abstract**

Measures obtained from diffusion-weighted imaging provide objective indices of white matter development and injury in the developing preterm brain. To date, diffusion tensor imaging (DTI) has been used widely, highlighting differences in fractional anisotropy (FA) and mean diffusivity (MD) between preterm infants at term and healthy term controls; altered white matter development associated with a number of perinatal risk factors; and correlations between FA values in the white matter in the neonatal period and subsequent neurodevelopmental outcome. Recent developments, including neurite orientation dispersion and density imaging (NODDI) and fixel-based analysis (FBA), enable white matter microstructure to be assessed in detail. Constrained spherical deconvolution (CSD) enables multiple fibre populations in an imaging voxel to be resolved and allows delineation of fibres that traverse regions of fibre-crossings, such as the arcuate fasciculus and cerebellar–cortical pathways. This review summarises DTI findings in the preterm brain and discusses initial findings in this population using CSD, NODDI, and FBA.

**Keywords**

infant, brain, diffusion magnetic resonance imaging

**Open Peer Review**

**Referee Status:**

	Invited Referees	
	1	2
<b>version 1</b> published 21 Aug 2018		

F1000 Faculty Reviews are commissioned from members of the prestigious F1000 Faculty. In order to make these reviews as comprehensive and accessible as possible, peer review takes place before publication; the referees are listed below, but their reports are not formally published.

- 1 **Risto A Kauppinen**, University of Bristol, UK
- 2 **Hao Huang**, Perelman School of Medicine, University of Pennsylvania, USA
- Qinlin Yu**, Perelman School of Medicine, University of Pennsylvania, USA

**Discuss this article**

Comments (0)

**Corresponding author:** Serena J. Counsell ([serena.counsell@kcl.ac.uk](mailto:serena.counsell@kcl.ac.uk))

**Author roles:** **Pecheva D:** Writing – Review & Editing; **Kelly C:** Writing – Review & Editing; **Kimpton J:** Writing – Review & Editing; **Bonthrone A:** Writing – Review & Editing; **Batalle D:** Writing – Review & Editing; **Zhang H:** Funding Acquisition, Supervision, Writing – Review & Editing; **Counsell SJ:** Funding Acquisition, Project Administration, Supervision, Writing – Original Draft Preparation, Writing – Review & Editing

**Competing interests:** No competing interests were disclosed.

**Grant information:** The authors receive funding from the Medical Research Council (MRC) UK (MR/L011530/1), the Biotechnology and Biological Sciences Research Council (grant number BB/J014567/1), the British Heart Foundation (FS/15/55/31649) and are supported by the Wellcome EPSRC Centre for Medical Engineering at King's College London (WT 203148/Z/16/Z), MRC strategic grant MR/K006355/1 and by the National Institute for Health Research (NIHR) Biomedical Research Centre based at Guy's and St Thomas' NHS Foundation Trust and King's College London.

*The funders had no role in study design, data collection and analysis, decision to publish, or preparation of the manuscript.*

**Copyright:** © 2018 Pecheva D *et al.* This is an open access article distributed under the terms of the [Creative Commons Attribution Licence](#), which permits unrestricted use, distribution, and reproduction in any medium, provided the original work is properly cited.

**How to cite this article:** Pecheva D, Kelly C, Kimpton J *et al.* **Recent advances in diffusion neuroimaging: applications in the developing preterm brain [version 1; referees: 2 approved]** *F1000Research* 2018, 7(F1000 Faculty Rev):1326 (doi: [10.12688/f1000research.15073.1](https://doi.org/10.12688/f1000research.15073.1))

**First published:** 21 Aug 2018, 7(F1000 Faculty Rev):1326 (doi: [10.12688/f1000research.15073.1](https://doi.org/10.12688/f1000research.15073.1))

## Introduction

Diffusion-weighted magnetic resonance imaging (dMRI) is a non-invasive imaging technique that measures the displacement of water molecules in tissue over time. As such, dMRI offers the opportunity to investigate tissue microstructure *in vivo* and provides quantitative measures that relate to brain injury and development. The most widely used dMRI analysis approach in the developing brain is diffusion tensor imaging (DTI), which has proven to be extremely useful for investigating brain development and injury. More recent approaches have moved beyond the tensor model to incorporate biophysical models to study tissue microstructure more specifically.

The aim of this review is to briefly describe studies assessing white and grey matter in the developing brain using advanced analysis approaches that have been used widely in the adult brain, such as neurite orientation dispersion and density imaging (NODDI), fixel-based analysis (FBA), and constrained spherical deconvolution (CSD). These approaches require high b-value (typically  $>2,000$  s/mm<sup>2</sup>), high angular resolution dMRI data which pose additional challenges in neonatal imaging including longer acquisition times, which may lead to motion corrupt data, reduced signal-to-noise ratio, and increased distortions. However, recent advances in data acquisition approaches and hardware, coupled with imaging at 3 Tesla, mean it is now possible to acquire high-quality HARDI data in the neonatal brain<sup>1</sup>. We believe these techniques will be increasingly used to improve our understanding of the neural substrate associated with impaired brain development in this population.

## Diffusion-weighted imaging

Diffusion is the constant motion of molecules due to thermal energy. Given an environment without restrictions, water molecules will traverse a random walk, with direction changes following collisions with other particles. However, in the

brain, the presence of axons, neuronal cell bodies, glial cells, and macromolecules comprise a heterogeneous environment which hinders and restricts diffusion. In the presence of these impediments, the measured root-mean-square displacement will be lower than predicted for water at room temperature. The term “apparent diffusion coefficient” is used to convey that the observed measure is influenced by the tissue microstructure. Diffusion is restricted if it is confined by physical boundaries, such as the diffusion of molecules in the intra-axonal space, causing the diffusion to become non-Gaussian<sup>2,3</sup>.

## Diffusion tensor imaging

The organisation of tissue microstructure will affect how water molecules diffuse. In a homogenous medium, the diffusion of water molecules is equal in all directions; this is isotropic diffusion. However, in a coherently organised microstructure, such as in white matter, diffusion is anisotropic<sup>4-6</sup>. Within white matter, water molecules diffuse more slowly perpendicular to the fibres than parallel to them (Figure 1). Under these conditions, the apparent diffusion coefficient will be different depending on the direction in which it is measured. To account for this, Basser *et al.*<sup>7</sup> proposed that diffusion is characterised using a mathematical tensor model. To examine water molecular motion in a tissue with an ordered microstructure using the tensor model, a minimum of six non-collinear directions of diffusion sensitisation is required, in addition to one with no diffusion weighting, although usually at least 30 unique sensitised directions are recommended to robustly estimate the tensor model parameters.

The diffusion tensor provides scalar, rotationally invariant indices<sup>8</sup>. Indices derived from  $\lambda_1, \lambda_2, \lambda_3$  (Figure 1) are, by definition, independent of orientation. The magnitude of the diffusivity along the main fibre orientation as estimated by DTI is given by  $\lambda_1$ , termed the axial diffusivity (AD). The average of the other

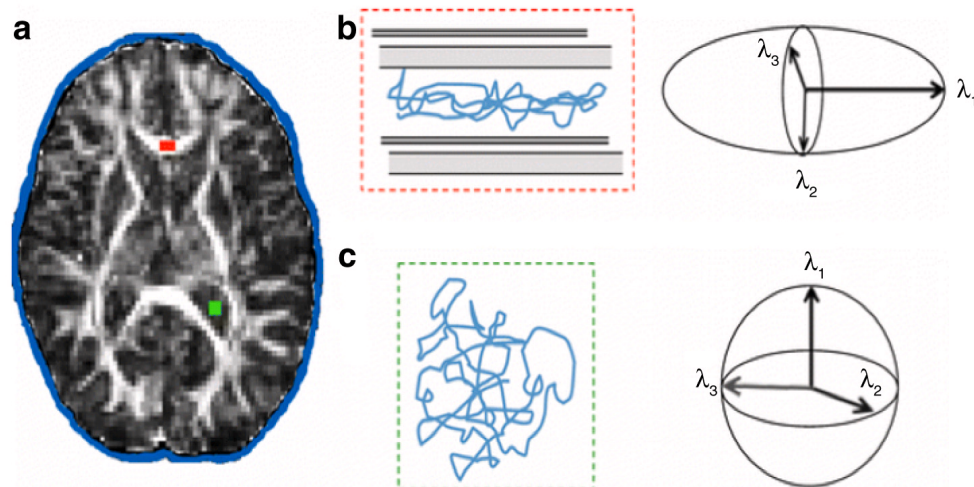


**Figure 1. Isotropic and anisotropic diffusion in the brain.** In the white matter of the corpus callosum (red), diffusion occurs preferentially along the axonal fibres, resulting in anisotropic diffusion (b). In the ventricular cerebrospinal fluid (CSF; green), diffusion is unhindered and can be described as isotropic (c). Diffusion tensor ellipsoids representing anisotropic and isotropic diffusion are shown in b and c, respectively. Reproduced with permission from 9.

two eigenvalues, the radial diffusivity (RD), describes the magnitude of diffusivity across the fibres. The mean diffusivity (MD) is the average of all three eigenvalues and provides a measure of the overall diffusivity within a voxel. Fractional anisotropy (FA) is the variance of the three eigenvalues normalised by the magnitude of the tensor and takes values between 0 and 1.

### DTI studies in the infant brain

The perinatal period is characterised by a pattern of decreasing MD, RD, and AD and increasing FA in the cerebral white matter in preterm infants<sup>10-14</sup> and term infants<sup>15,16</sup>. White matter maturation follows a heterogeneous spatiotemporal pattern, with different fasciculi maturing at different times and different rates<sup>15-23</sup> in a posterior-to-anterior and a central-to-peripheral direction of maturation. The increase in FA takes place before myelin is evident histologically and is attributed to changes in white matter structure which accompany the premyelinating state including an increase in axonal membrane maturation and microtubule-associated proteins, a change in axon caliber, and an increase in oligodendrocyte number<sup>24-26</sup>. At this stage, the highest FA values are seen in the unmyelinated but highly organised commissural fibres in the splenium and genu of the corpus callosum. The second stage is associated with the histological appearance of myelin and subsequent maturation, with the earliest signs observed in the projection fibres of the posterior limb of the internal capsule around term<sup>27</sup>.

Lower FA and increased MD are found across the white matter in preterm infants compared with term-born infants<sup>24,28-30</sup>, and increased prematurity is associated with lower FA and higher MD<sup>13,31-35</sup>. Furthermore, infants with white matter injury identified on conventional MRI show reduced anisotropy and increased MD and RD across the white matter in comparison to preterm infants with normal MRI<sup>14,36-40</sup>. White matter diffusion measures in preterm infants at term equivalent age have been related to subsequent neurodevelopmental performance. Increased FA and decreased MD and RD in the white matter at term equivalent age are associated with improved motor, cognitive, and language performance in early childhood<sup>41-47</sup> and improved visual function<sup>48-50</sup>.

In addition to assessing white matter, DTI studies of cortical grey matter have identified altered cortical development in infants born preterm. Cortical maturation up to term equivalent age is characterised by decreasing FA and MD, reflecting increased dendritic arborisation and synapse formation<sup>35,51-53</sup>. FA and MD are elevated in preterm infants at term equivalent age compared to infants born at term, suggesting impaired cortical development in this population<sup>52</sup>.

### Limitations of DTI

While DTI has proven to be a powerful technique for studying the brain, a major limitation is that it is only able to depict a single fibre population within a voxel. DTI fails to represent appropriately the tissue microstructure in the presence of crossing fibres and DTI-derived measures lack tissue specificity, as these measures can be affected by multiple microstructural features. Moreover, in a restricted environment, diffusion is no longer Gaussian and the tensor model deviates from the signal.

The use of more advanced analysis approaches, such as those that enable microstructure to be studied with greater specificity, require high angular resolution diffusion imaging (HARDI) acquisitions at a higher b-value than has typically been used in the neonatal brain. These approaches have long acquisition times and so their use in unseeded neonates has been limited. However, advances in MRI acquisition techniques, such as the use of protocols designed specifically for neonates using neonatal head coils and multiband MRI coupled with modern gradient coil systems, with maximum gradient amplitude, slew rate, and duty cycle<sup>1,54</sup>, now enable HARDI data to be acquired in a clinically feasible time.

### Compartment models of microstructure

Compartment models provide a biophysical interpretation of the diffusion-weighted signal and attempt to characterise the complexity of cerebral tissue by decomposing the signal into compartments describing diffusion within distinct microstructural constituents.

Stanisz *et al.*<sup>55</sup> first introduced the three-compartment model comprising a restricted intra-axonal compartment, anisotropic hindered extra-axonal compartment, and a restricted isotropic compartment describing diffusion within cellular structures such as glial cells. Behrens *et al.*<sup>56</sup> presented a method to account for multiple fibre populations using the ball and stick model where diffusion along axons is represented by sticks and outside the axons diffusion is an isotropic ball. CHARMED<sup>57</sup> models the intra-axonal space using cylinders with a distribution of radii given by the  $\Gamma$ -distribution and extra-axonal space as tensor with a principle direction aligned with the cylinders. This was extended to provide an estimate of axon diameter in the AxCaliber framework<sup>58,59</sup>. Alexander<sup>60</sup> simplified CHARMED by using a single axon radius and symmetric tensor that was used in the ActiveAx framework to estimate axon diameter in biological tissue<sup>61,62</sup> and axon diameter mapping in the presence of orientation dispersion<sup>63</sup>. However, recent work shows that the gradient amplitudes attainable with current clinical scanners are not able to estimate axon diameter accurately<sup>64,65</sup>.

NODDI<sup>66</sup> provides measures of neurite density index (NDI) and orientation dispersion index (ODI). The model consists of three compartments modelling the intracellular, extracellular, and cerebrospinal fluid (CSF) environments. The intraneurite compartment captures the diffusion inside dendrites and axons, collectively termed neurites. The intraneurite compartment is modelled using sticks to represent unhindered diffusion along the neurites and highly restricted diffusion perpendicular to the neurites. The orientation distribution can vary from being highly parallel, reflecting the coherent organisation of white matter fibres such as in the posterior limb of the internal capsule or the corpus callosum, to highly dispersed, such as in regions of crossing fibres like the centrum semiovale or the complex configuration of the cortex. The extraneurite compartment represents the space occupied by glial cells and neuronal somas where diffusion is hindered and is modelled as an anisotropic Gaussian distribution using a zeppelin. The CSF compartment is modelled as isotropic Gaussian diffusion.

The NODDI model has been applied to investigate white and grey matter maturation in the preterm brain<sup>34,67,68</sup>. NDI increases in the white matter with increasing maturation, with the highest NDI values observed in primary motor and somatosensory tracts and lower values observed in association fibres<sup>67,69</sup>. Combined with graph theoretical approaches and network-based analysis, both FA- and NDI-weighted connections were highly correlated with age at MRI in a widespread pattern encompassing most white matter connections between 25 and 45 weeks post-menstrual age (PMA). Lower gestational age (GA) at birth was significantly correlated with lower FA and NDI, and we observed a consistent negative correlation of relative NDI-weighted global efficiency with GA at birth, suggesting an alteration in network topology with increased prematurity at birth<sup>67</sup>. Cortical grey matter maturation is characterised by increasing ODI (accompanied

by decreasing MD and FA), reflecting increased dendritic arborisation. At around 38 weeks' GA, this increase in ODI plateaued, but after this period NDI increased in primary motor and sensory regions (Figure 2), suggesting that cortical development up to 38 weeks' PMA shows a predominant increase in dendritic arborisation and neurite growth, while after 38 weeks' PMA it is dominated by increasing cellular and organelle density<sup>34</sup>.

The DIAMOND model<sup>70</sup> combines compartmental and statistical modelling to represent restricted, hindered, and isotropic compartments using three peak-shaped matrix-variate distributions. DIAMOND estimates the number of tissue compartments in each voxel and provides compartment-specific measures of FA, AD, RD, and MD and a measure of heterogeneity within

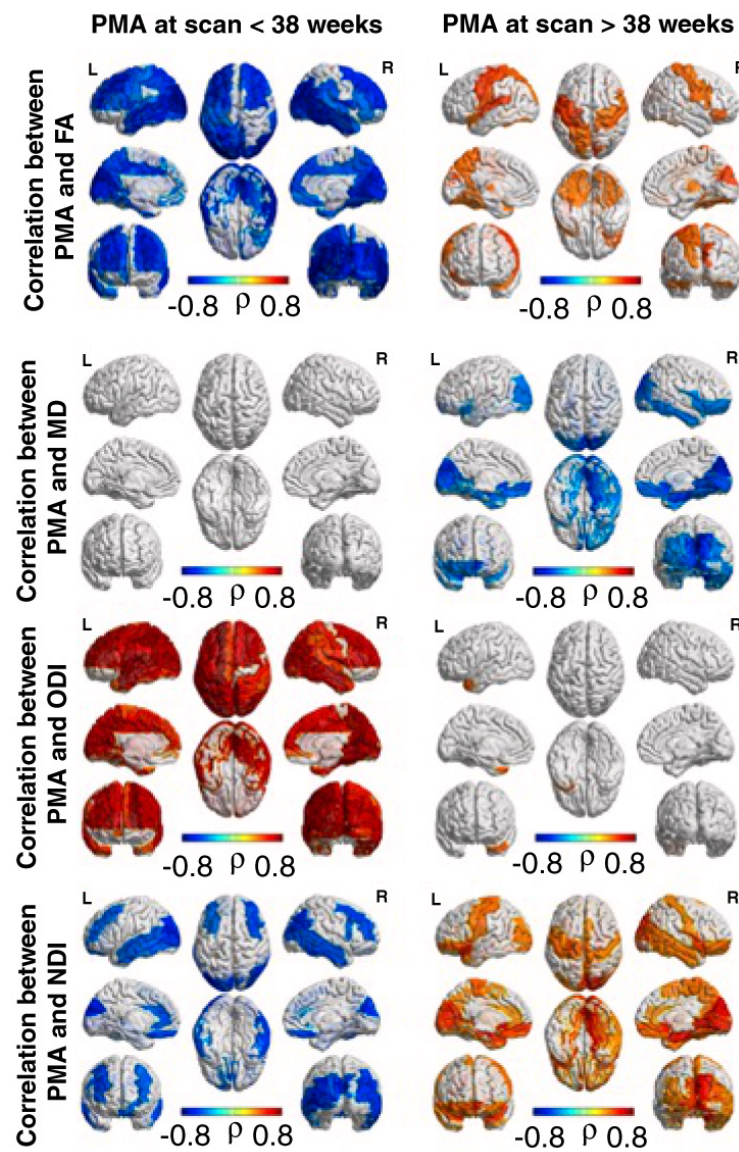


**Figure 2. Correlation between cortical diffusion characteristics and age at scan.** Hot colours indicate increase and cool colours indicate decrease in diffusion measure. Abbreviations: FA, fractional anisotropy; MD, mean diffusivity; NDI, neurite density index; ODI, orientation dispersion index; PMA, post-menstrual age. Reproduced from <sup>34</sup>.

the compartment. This model was recently applied to assess cortical maturation in the preterm cortex, demonstrating a decrease in the radial organisation of the cortex<sup>71</sup>.

Approaches to model the diffusion signal have limitations, including assuming non-exchanging tissue compartments and fixed compartmental diffusivities<sup>72</sup>, and, to date, there have been no studies validating these measures with human preterm or neonatal tissue samples. However, ODI measures have recently been correlated with changes in neurite geometrical configuration assessed with histology in a population with spinal cord multiple sclerosis<sup>73</sup>, suggesting that model indices are relevant proxies of underlying microstructure.

### Constrained spherical deconvolution

CSD estimates the fibre orientation distribution (FOD) in the presence of multiple fibre orientations<sup>74–78</sup>. It was initially introduced for single-shell HARDI data<sup>79</sup> and is able to estimate FODs regardless of the number of fibre populations within a voxel. It is assumed that each fibre bundle has the same diffusion properties, apart from the orientation, and that no exchange occurs between bundles over the time-scale of DWI acquisition. The signal emanating from each fibre bundle is independent and they can be summed. The diffusion-attenuated profile for an anisotropic fibre bundle is represented by a response function. The response function is low amplitude along the axis, where diffusion is high, and high amplitude in the radial plane, where diffusion is low. Recently, multi-tissue CSD has been introduced, which exploits the different diffusion dependencies of different tissues at multiple b-values (b-value refers to the

degree of diffusion weighting which is related to the amplitude and duration of the diffusion gradients and the time interval between the leading edges of the two pulsed gradients) to derive tissue-specific response functions, where grey matter and CSF response functions are both isotropic, leading to improved estimation of the FOD<sup>80</sup>.

CSD-based tractography has been used in a limited number of studies in the infant brain to visualise fibre bundles that are not readily delineated using DTI-based approaches. In Pieterman *et al.*<sup>81</sup>, we were able to visualise cerebellar–cortical pathways crossing in the mid-brain (Figure 3). In another recent study, we were able to delineate the arcuate fasciculus, which traverses regions of fibre crossings in the centrum semiovale and we observed that FA values of the arcuate fasciculus in preterm infants at term equivalent age correlated with language performance at 2 years (Figure 4)<sup>82</sup>.

### Fixel-based analysis

CSD has led to the development of fibre bundle-specific measures. Raffelt *et al.*<sup>83</sup> introduced a measure of apparent fibre density (AFD) of individual fibre populations estimated from the FOD. A fixel describes an individual different fibre bundle within an imaging voxel where fibre bundles of different orientations may be present in an imaging voxel. AFD is based on the assumptions that the intra-axonal water diffusion is restricted in the direction perpendicular to the fibre orientation, the extra-axonal diffusion-weighted signal is attenuated at high b-values (>2,000 s/mm<sup>2</sup>), and the diffusion-weighted signal from the restricted compartment is preserved under

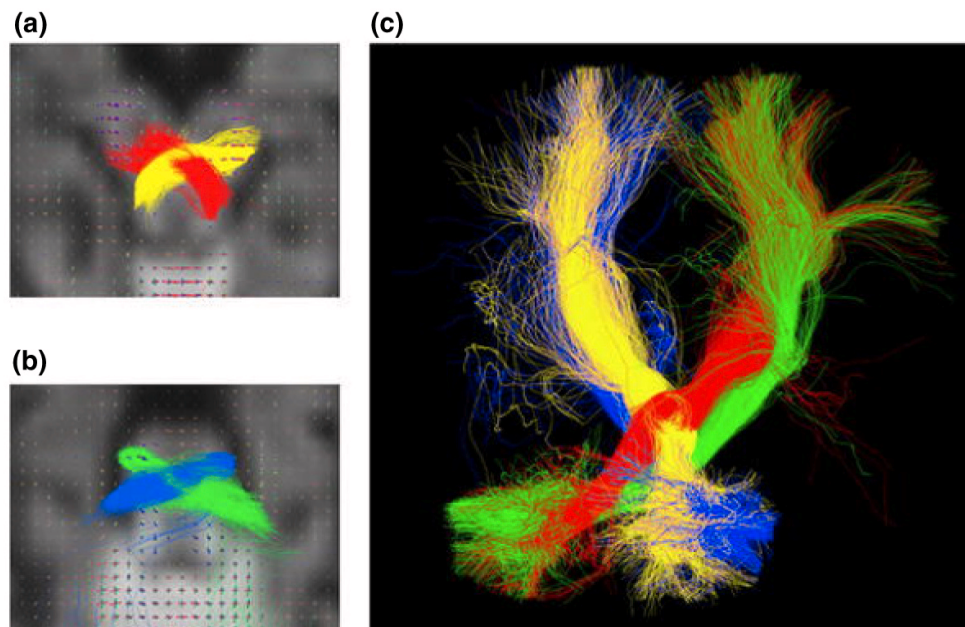


**Figure 3.** Reconstruction of cerebello–thalamo–cortical tract (CTC, red-yellow) and cortico–ponto–cerebellar tract (CPC, blue-green) in an infant born at 33 weeks and imaged at 40 weeks post-menstrual age with fibre orientation distribution plots overlaid on the diffusion data. (a) Crossing fibres of the CTC tract at the level of the mesencephalon. (b) Crossing fibres of the CPC tract at the level of the pons. (c) 3D reconstruction of both tracts. Reproduced from 81.

typical diffusion-weighted gradient pulse durations used *in vivo*. Consequently, the radial diffusion-weighted signal is approximately proportional to the volume of the intra-axonal compartment<sup>83</sup>. Since the FOD amplitude is proportional to the radial diffusion-weighted signal, it provides a measure of fibre density (FD) determined as a proportion of the volume occupied by the fibre population<sup>83</sup>, as illustrated by Figure 5. This measure would detect within-voxel changes related to the volume of restricted water along a specific direction. AFD also accounts for differences in macroscopic white matter structure across subjects. FODs are modulated according to changes in local volume, such as expansion or contraction, that occur during registration. This presents a measure pertaining to both microscopic changes in FD and macroscopic morphological changes that occur across voxels.

Raffelt *et al.*<sup>84</sup> make a distinction between the changes in microstructure that occur within a voxel and the macroscopic changes in morphology that occur across voxels. They introduced a measure of FD derived solely from unmodulated FOD amplitude so as to describe changes in white matter microstructure without the effects of macroscopic morphological changes. Changes in white matter microstructure which would result in a reduction in FD can be visualised in Figure 6. Nonetheless, macroscopic alterations in morphology are likely to occur across white matter during development and need to be accounted for. Raffelt *et al.*<sup>84</sup> provide, in addition to FD, a measure of macroscopic differences in morphology based on the local deformations that are applied during registration. Changes in brain morphology have previously been investigated using voxel-based morphometry (VBM)<sup>85</sup> and tensor-based morphometry<sup>86,87</sup>. Local changes

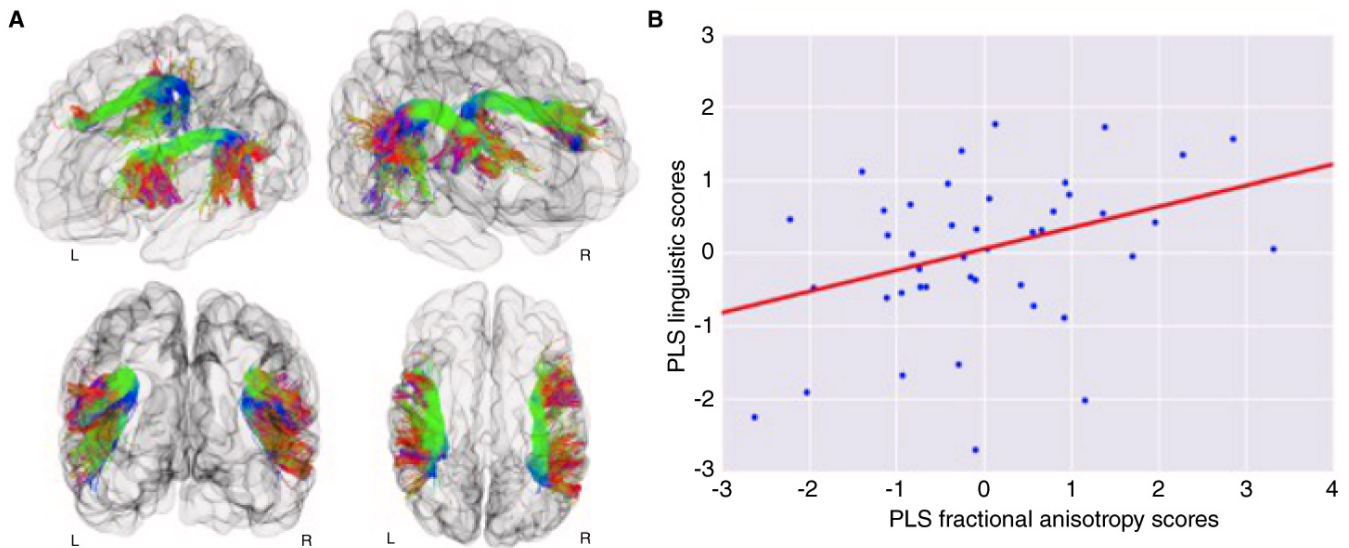


**Figure 4.** Inter-subject differences in linguistic performance at two years were associated with term equivalent fractional anisotropy (FA) of the left and right arcuate fasciculus independently of degree of prematurity. (a) Visualisation of an infant brain and the reconstructed arcuate fasciculi from left-frontal, right-frontal, frontal, and top view. The tracts are coloured by direction: green for anterior-posterior, red for left-right, and blue for superior-inferior. (b) Using cross-validated partial-least-square (PLS) regression, one statistically significant mode of brain-behaviour covariation between PLS FA scores and PLS language scores was identified ( $r = 0.36$ ; family-wise error [FWE]-corrected  $P$ -value = 0.0110). Term equivalent FA of the left and right arcuate fasciculi was associated with individual differences in composite linguistic skills in early childhood. This link was still present even when controlling for degree of premature delivery measured by gestational age (GA) at birth ( $r = 0.32$ , FWE-corrected  $P$ -value = 0.0230). Reproduced from 82.

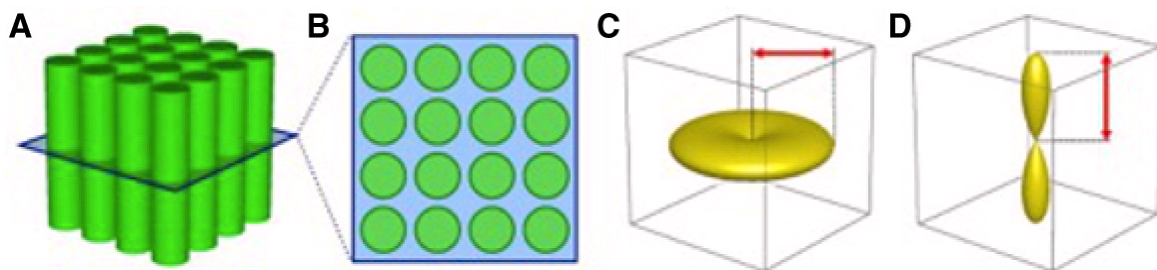


**Figure 5.** A single fibre population within a voxel (A, B), the expected diffusion-weighted signal profile (C), and the associated fibre orientation distribution (FOD) (D). The FOD amplitude is proportional to the radial signal profile and therefore the fibre density of the fibre population. Image adapted from 88.

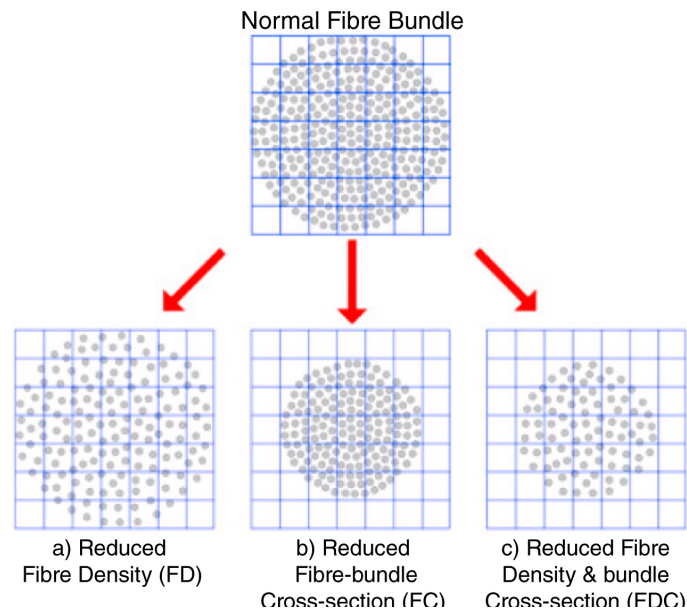


**Figure 6. A schematic representation of a fibre bundle cross-section made of numerous axons (grey circles).** Anterior commissure voxels represented by the grid. Panels (a), (b), and (c) describe three different ways in which a fibre bundle can change: (a) a reduction in within-voxel fibre density, (b) a macroscopic change in fibre-cross section across voxels, and (c) a combination of reductions in both fibre density and cross-section. Image adapted from 84.

in volume can be investigated using the information from a subject's nonlinear deformation to a template. At each voxel, the determinant of the Jacobian describes the expansion or contraction of the subject image relative to a target. This method focuses on the changes in fibre bundle that occur perpendicular to the main fibre orientation, as a reduced fibre bundle cross-section would imply a reduced number of axons. Using FOD registration, it is possible to assess changes in volume with respect to specific fibre orientations. This provides a fibre bundle-specific measure of fibre cross-section (FC) based on the Jacobian determinant following registration of FOD images.

To date, there have been few studies assessing white matter in the preterm brain using FBA. Pannek *et al.* demonstrated reduced FD, FC, and FD multiplied by FC (FDC) in the corticospinal tract and corpus callosum in preterm infants at term equivalent age compared to healthy controls<sup>89</sup>. We have observed a significant negative correlation between FC and FDC and duration of mechanical ventilation and parenteral nutrition in preterm infants at term equivalent age, suggesting that aberrant white matter development previously attributed to microstructural changes may be due to alterations in the size (fibre cross-sectional area) of specific fibre bundles at the macroscopic scale<sup>90</sup>.

## Summary

Recent advances in diffusion acquisition and analysis approaches enable white and grey matter microstructure to be probed in detail, demonstrating increases in NDI and FC in white matter and increasing ODI in cortical grey matter with increasing maturation. CSD-based tractography facilitates the delineation of

complex fibre bundles that have not been clearly depicted using DTI approaches. Large-scale studies (such as the developing Human Connectome Project, <http://www.developingconnectome.org>) are now underway and are obtaining high b-value HARDI data in the neonatal brain with the aim of improving our understanding of human brain development and the impact of environmental and genetic factors on brain development. It is likely that the acquisition and analysis techniques outlined in this review will be confined to the research environment in the short term. However, the ultimate aim of neonatal neuroimaging is to facilitate early diagnosis and prognosis, and innovations in image acquisition including multiband techniques to reduce acquisition time are likely to facilitate the increased use of these advanced methods in the neonatal brain in the future.

## Grant information

The authors receive funding from the Medical Research Council (MRC) UK (MR/L011530/1), the Biotechnology and Biological Sciences Research Council (grant number [BB/J014567/1](#)), the British Heart Foundation (FS/15/55/31649) and are supported by the Wellcome EPSRC Centre for Medical Engineering at King's College London (WT 203148/Z/16/Z), MRC strategic grant MR/K006355/1 and by the National Institute for Health Research (NIHR) Biomedical Research Centre based at Guy's and St Thomas' NHS Foundation Trust and King's College London.

*The funders had no role in study design, data collection and analysis, decision to publish, or preparation of the manuscript.*



## References



1. **F** Hutter J, Tournier JD, Price AN, *et al.*: **Time-efficient and flexible design of optimized multishell HARDI diffusion.** *Magn Reson Med.* 2018; 79(3): 1276–92. [PubMed Abstract](#) | [Publisher Full Text](#) | [Free Full Text](#) | [F1000 Recommendation](#)
2. Assaf Y, Freidlin RZ, Rohde GK, *et al.*: **New modeling and experimental framework to characterize hindered and restricted water diffusion in brain white matter.** *Magn Reson Med.* 2004; 52(5): 965–78. [PubMed Abstract](#) | [Publisher Full Text](#)
3. Basser PJ: **Inferring microstructural features and the physiological state of tissues from diffusion-weighted images.** *NMR Biomed.* 1995; 8(7–8): 333–44. [PubMed Abstract](#) | [Publisher Full Text](#)
4. Hajnal JV, Doran M, Hall AS, *et al.*: **MR imaging of anisotropically restricted diffusion of water in the nervous system: technical, anatomic, and pathologic considerations.** *J Comput Assist Tomogr.* 1991; 15(1): 1–18. [PubMed Abstract](#)
5. Moseley ME, Cohen Y, Kucharczyk J, *et al.*: **Diffusion-weighted MR imaging of anisotropic water diffusion in cat central nervous system.** *Radiology.* 1990; 176(2): 439–45. [PubMed Abstract](#) | [Publisher Full Text](#)
6. Thomsen C, Henriksen O, Ring P: **In vivo measurement of water self diffusion in the human brain by magnetic resonance imaging.** *Acta Radiol.* 1987; 28(3): 353–61. [PubMed Abstract](#) | [Publisher Full Text](#)
7. Basser PJ, Mattiello J, LeBihan D: **MR diffusion tensor spectroscopy and imaging.** *Biophys J.* 1994; 66(1): 259–67. [PubMed Abstract](#) | [Publisher Full Text](#) | [Free Full Text](#)
8. Pierpaoli C, Basser PJ: **Toward a quantitative assessment of diffusion anisotropy.** *Magn Reson Med.* 1996; 36(6): 893–906. [PubMed Abstract](#) | [Publisher Full Text](#)
9. Pandit AS, Ball G, Edwards AD, *et al.*: **Diffusion magnetic resonance imaging in preterm brain injury.** *Neuroradiology.* 2013; 55 Suppl 2: 65–95. [PubMed Abstract](#) | [Publisher Full Text](#)
10. de Bruine FT, van Wezel-Meijler G, Leijser LM, *et al.*: **Tractography of developing white matter of the internal capsule and corpus callosum in very preterm infants.** *Eur Radiol.* 2011; 21(3): 538–47. [PubMed Abstract](#) | [Publisher Full Text](#) | [Free Full Text](#)
11. Kersbergen KJ, Leemans A, Groenendaal F, *et al.*: **Microstructural brain development between 30 and 40 weeks corrected age in a longitudinal cohort of extremely preterm infants.** *NeuroImage.* 2014; 103: 214–24. [PubMed Abstract](#) | [Publisher Full Text](#)
12. Miller SP, Vigneron DB, Henry RG, *et al.*: **Serial quantitative diffusion tensor MRI of the premature brain: development in newborns with and without injury.** *J Magn Reson Imaging.* 2002; 16(6): 621–32. [PubMed Abstract](#) | [Publisher Full Text](#)
13. Partridge SC, Mukherjee P, Henry RG, *et al.*: **Diffusion tensor imaging: serial quantitation of white matter tract maturity in premature newborns.** *NeuroImage.* 2004; 22(3): 1302–14. [PubMed Abstract](#) | [Publisher Full Text](#)
14. van Pul C, van Kooij BJ, de Vries LS, *et al.*: **Quantitative fiber tracking in the corpus callosum and internal capsule reveals microstructural abnormalities in preterm infants at term-equivalent age.** *AJNR Am J Neuroradiol.* 2012; 33(4): 678–84. [PubMed Abstract](#) | [Publisher Full Text](#)
15. Dubois J, Hertz-Pannier L, Dehaene-Lambertz G, *et al.*: **Assessment of the early organization and maturation of infants' cerebral white matter fiber bundles: a feasibility study using quantitative diffusion tensor imaging and tractography.** *NeuroImage.* 2006; 30(4): 1121–32. [PubMed Abstract](#) | [Publisher Full Text](#)
16. Oishi K, Mori S, Donohue PK, *et al.*: **Multi-contrast human neonatal brain atlas: application to normal neonate development analysis.** *NeuroImage.* 2011; 56(1): 8–20. [PubMed Abstract](#) | [Publisher Full Text](#) | [Free Full Text](#)
17. Braga RM, Roze E, Ball G, *et al.*: **Development of the Corticospinal and Callosal Tracts from Extremely Premature Birth up to 2 Years of Age.** *PLoS One.* 2015; 10(5): e0125681. [PubMed Abstract](#) | [Publisher Full Text](#) | [Free Full Text](#)
18. Dubois J, Dehaene-Lambertz G, Perrin M, *et al.*: **Asynchrony of the early maturation of white matter bundles in healthy infants: quantitative landmarks revealed noninvasively by diffusion tensor imaging.** *Hum Brain Mapp.* 2008; 29(1): 14–27. [PubMed Abstract](#) | [Publisher Full Text](#)
19. Gao W, Lin W, Chen Y, *et al.*: **Temporal and spatial development of axonal maturation and myelination of white matter in the developing brain.** *AJNR Am J Neuroradiol.* 2009; 30(2): 290–6. [PubMed Abstract](#) | [Publisher Full Text](#) | [Free Full Text](#)
20. Kulikova S, Hertz-Pannier L, Dehaene-Lambertz G, *et al.*: **Multi-parametric evaluation of the white matter maturation.** *Brain Struct Funct.* 2015; 220(6): 3657–72. [PubMed Abstract](#) | [Publisher Full Text](#) | [Free Full Text](#)
21. Nossin-Manor R, Card D, Morris D, *et al.*: **Quantitative MRI in the very preterm brain: assessing tissue organization and myelination using magnetization transfer, diffusion tensor and T<sub>2</sub> imaging.** *NeuroImage.* 2013; 64: 505–16. [PubMed Abstract](#) | [Publisher Full Text](#)
22. Nossin-Manor R, Card D, Raybaud C, *et al.*: **Cerebral maturation in the early preterm period-A magnetization transfer and diffusion tensor imaging study using voxel-based analysis.** *NeuroImage.* 2015; 112: 30–42. [PubMed Abstract](#) | [Publisher Full Text](#)
23. Rose J, Vassar R, Cahill-Rowley K, *et al.*: **Brain microstructural development at near-term age in very-low-birth-weight preterm infants: an atlas-based diffusion imaging study.** *NeuroImage.* 2014; 86: 244–56. [PubMed Abstract](#) | [Publisher Full Text](#) | [Free Full Text](#)
24. Hüppi PS, Warfield S, Kikinis R, *et al.*: **Quantitative magnetic resonance imaging of brain development in premature and mature newborns.** *Ann Neurol.* 1998; 43(2): 224–35. [PubMed Abstract](#) | [Publisher Full Text](#)
25. Wimberger DM, Roberts TP, Barkovich AJ, *et al.*: **Identification of "premyelination" by diffusion-weighted MRI.** *J Comput Assist Tomogr.* 1995; 19(1): 28–33. [PubMed Abstract](#) | [Publisher Full Text](#)
26. Neil JJ, Shiran SI, McKinstry RC, *et al.*: **Normal brain in human newborns: apparent diffusion coefficient and diffusion anisotropy measured by using diffusion tensor MR imaging.** *Radiology.* 1998; 209(1): 57–66. [PubMed Abstract](#) | [Publisher Full Text](#)
27. Brody BA, Kinney HC, Kloman AS, *et al.*: **Sequence of central nervous system myelination in human infancy. I. An autopsy study of myelination.** *J Neuropathol Exp Neurol.* 1987; 46(3): 283–301. [PubMed Abstract](#) | [Publisher Full Text](#)
28. Anjari M, Srinivasan L, Allsop JM, *et al.*: **Diffusion tensor imaging with tract-based spatial statistics reveals local white matter abnormalities in preterm infants.** *NeuroImage.* 2007; 35(3): 1021–7. [PubMed Abstract](#) | [Publisher Full Text](#)
29. Rose SE, Hatzigeorgiou X, Strudwick MW, *et al.*: **Altered white matter diffusion anisotropy in normal and preterm infants at term-equivalent age.** *Magn Reson Med.* 2008; 60(4): 761–7. [PubMed Abstract](#) | [Publisher Full Text](#)
30. Thompson DK, Inder TE, Faggian N, *et al.*: **Characterization of the corpus callosum in very preterm and full-term infants utilizing MRI.** *NeuroImage.* 2011; 55(2): 479–90. [PubMed Abstract](#) | [Publisher Full Text](#) | [Free Full Text](#)
31. Ball G, Counsell SJ, Anjari M, *et al.*: **An optimised tract-based spatial statistics protocol for neonates: applications to prematurity and chronic lung disease.** *NeuroImage.* 2010; 53(1): 94–102. [PubMed Abstract](#) | [Publisher Full Text](#)
32. Hasegawa T, Yamada K, Morimoto M, *et al.*: **Development of corpus callosum in preterm infants is affected by the prematurity: in vivo assessment of diffusion tensor imaging at term-equivalent age.** *Pediatr Res.* 2011; 69(3): 249–54. [PubMed Abstract](#) | [Publisher Full Text](#)
33. Huang H, Zhang J, Wakana S, *et al.*: **White and gray matter development in human fetal, newborn and pediatric brains.** *NeuroImage.* 2006; 33(1): 27–38. [PubMed Abstract](#) | [Publisher Full Text](#)
34. Bataille D, O'Muircheartaigh J, Makropoulos A, *et al.*: **Different patterns of cortical maturation before and after 38 weeks gestational age demonstrated by diffusion MRI in vivo.** *NeuroImage.* 2018; pii: S1053-8119(18)30460-9. [PubMed Abstract](#) | [Publisher Full Text](#)
35. **F** Ouyang M, Dubois J, Yu Q, *et al.*: **Delineation of early brain development from fetuses to infants with diffusion MRI and beyond.** *NeuroImage.* 2018; pii: S1053-8119(18)30301-X. [PubMed Abstract](#) | [Publisher Full Text](#) | [F1000 Recommendation](#)
36. Cheong JL, Thompson DK, Wang HX, *et al.*: **Abnormal white matter signal on MR imaging is related to abnormal tissue microstructure.** *AJNR Am J Neuroradiol.* 2009; 30(3): 623–8. [PubMed Abstract](#) | [Publisher Full Text](#)
37. Counsell SJ, Allsop JM, Harrison MC, *et al.*: **Diffusion-weighted imaging of the brain in preterm infants with focal and diffuse white matter abnormality.** *Pediatrics.* 2003; 112(1 Pt 1): 1–7. [PubMed Abstract](#)
38. Counsell SJ, Shen Y, Boardman JP, *et al.*: **Axial and radial diffusivity in preterm infants who have diffuse white matter changes on magnetic resonance imaging at term-equivalent age.** *Pediatrics.* 2006; 117(2): 376–86. [PubMed Abstract](#) | [Publisher Full Text](#)
39. Hüppi PS, Murphy B, Maier SE, *et al.*: **Microstructural brain development after perinatal cerebral white matter injury assessed by diffusion tensor magnetic resonance imaging.** *Pediatrics.* 2001; 107(3): 455–60. [PubMed Abstract](#) | [Publisher Full Text](#)
40. Liu Y, Aeby A, Balériaux D, *et al.*: **White matter abnormalities are related to microstructural changes in preterm neonates at term-equivalent age: a diffusion tensor imaging and probabilistic tractography study.** *AJNR Am J Neuroradiol.* 2012; 33(5): 839–45. [PubMed Abstract](#) | [Publisher Full Text](#)
41. Counsell SJ, Edwards AD, Chew AT, *et al.*: **Specific relations between neurodevelopmental abilities and white matter microstructure in children born**

- preterm. *Brain*. 2008; 131(Pt 12): 3201–8.  
[PubMed Abstract](#) | [Publisher Full Text](#)
42. De Bruïne FT, van Wezel-Meijjer G, Leijser LM, *et al.*: Tractography of white-matter tracts in very preterm infants: a 2-year follow-up study. *Dev Med Child Neurol*. 2013; 55(5): 427–33.  
[PubMed Abstract](#) | [Publisher Full Text](#)
43. Duerden EG, Foong J, Chau V, *et al.*: Tract-Based Spatial Statistics in Preterm-Born Neonates Predicts Cognitive and Motor Outcomes at 18 Months. *AJNR Am J Neuroradiol*. 2015; 36(8): 1565–71.  
[PubMed Abstract](#) | [Publisher Full Text](#)
44. Krishnan ML, Dyet LE, Boardman JP, *et al.*: Relationship between white matter apparent diffusion coefficients in preterm infants at term-equivalent age and developmental outcome at 2 years. *Pediatrics*. 2007; 120(3): e604–9.  
[PubMed Abstract](#) | [Publisher Full Text](#)
45. Rose J, Mirmiran M, Butler EE, *et al.*: Neonatal microstructural development of the internal capsule on diffusion tensor imaging correlates with severity of gait and motor deficits. *Dev Med Child Neurol*. 2007; 49(10): 745–50.  
[PubMed Abstract](#) | [Publisher Full Text](#)
46. van Kooij BJ, de Vries LS, Ball G, *et al.*: Neonatal tract-based spatial statistics findings and outcome in preterm infants. *AJNR Am J Neuroradiol*. 2012; 33(1): 188–94.  
[PubMed Abstract](#) | [Publisher Full Text](#)
47. Barnett ML, Tumor N, Ball G, *et al.*: Exploring the multiple-hit hypothesis of preterm white matter damage using diffusion MRI. *NeuroImage Clin*. 2017; 17: 596–606.  
[PubMed Abstract](#) | [Publisher Full Text](#) | [Free Full Text](#)
48. Bassi L, Ricci D, Volzone A, *et al.*: Probabilistic diffusion tractography of the optic radiations and visual function in preterm infants at term equivalent age. *Brain*. 2008; 131(Pt 2): 573–82.  
[PubMed Abstract](#) | [Publisher Full Text](#)
49. Berman JJ, Glass HC, Miller SP, *et al.*: Quantitative fiber tracking analysis of the optic radiation correlated with visual performance in premature newborns. *AJNR Am J Neuroradiol*. 2009; 30(1): 120–4.  
[PubMed Abstract](#) | [Publisher Full Text](#) | [Free Full Text](#)
50. Groppo M, Ricci D, Bassi L, *et al.*: Development of the optic radiations and visual function after premature birth. *Cortex*. 2014; 56: 30–7.  
[PubMed Abstract](#) | [Publisher Full Text](#)
51. McKinsty RC, Mathur A, Miller JH, *et al.*: Radial organization of developing preterm human cerebral cortex revealed by non-invasive water diffusion anisotropy MRI. *Cereb Cortex*. 2002; 12(12): 1237–43.  
[PubMed Abstract](#) | [Publisher Full Text](#)
52. Ball G, Srinivasan L, Aljabar P, *et al.*: Development of cortical microstructure in the preterm human brain. *Proc Natl Acad Sci U S A*. 2013; 110(23): 9541–6.  
[PubMed Abstract](#) | [Publisher Full Text](#) | [Free Full Text](#)
53. F Yu Q, Ouyang A, Chalak L, *et al.*: Structural Development of Human Fetal and Preterm Brain Cortical Plate Based on Population-Averaged Templates. *Cereb Cortex*. 2016; 26(11): 4381–91.  
[PubMed Abstract](#) | [Publisher Full Text](#) | [Free Full Text](#) | [F1000 Recommendation](#)
54. Hughes EJ, Winchman T, Padormo F, *et al.*: A dedicated neonatal brain imaging system. *Magn Reson Med*. 2017; 78(2): 794–804.  
[PubMed Abstract](#) | [Publisher Full Text](#) | [Free Full Text](#)
55. Stanisz GJ, Szafer A, Wright GA, *et al.*: An analytical model of restricted diffusion in bovine optic nerve. *Magn Reson Med*. 1997; 37(1): 103–11.  
[PubMed Abstract](#) | [Publisher Full Text](#)
56. Behrens TE, Woolrich MW, Jenkinson M, *et al.*: Characterization and propagation of uncertainty in diffusion-weighted MR imaging. *Magn Reson Med*. 2003; 50(5): 1077–88.  
[PubMed Abstract](#) | [Publisher Full Text](#)
57. Assaf Y, Basser PJ: Composite hindered and restricted model of diffusion (CHARMED) MR imaging of the human brain. *NeuroImage*. 2005; 27(1): 48–58.  
[PubMed Abstract](#) | [Publisher Full Text](#)
58. Assaf Y, Blumenfeld-Katzir T, Yovel Y, *et al.*: AxCaliber: a method for measuring axon diameter distribution from diffusion MRI. *Magn Reson Med*. 2008; 59(6): 1347–54.  
[PubMed Abstract](#) | [Publisher Full Text](#) | [Free Full Text](#)
59. Barazany D, Basser PJ, Assaf Y: *In vivo* measurement of axon diameter distribution in the corpus callosum of rat brain. *Brain*. 2009; 132(Pt 5): 1210–20.  
[PubMed Abstract](#) | [Publisher Full Text](#) | [Free Full Text](#)
60. Alexander DC: A general framework for experiment design in diffusion MRI and its application in measuring direct tissue-microstructure features. *Magn Reson Med*. 2008; 60(2): 439–48.  
[PubMed Abstract](#) | [Publisher Full Text](#)
61. Alexander DC, Hubbard PL, Hall MG, *et al.*: Orientationally invariant indices of axon diameter and density from diffusion MRI. *NeuroImage*. 2010; 52(4): 1374–89.  
[PubMed Abstract](#) | [Publisher Full Text](#)
62. Dyrby TB, Sogaard LV, Hall MG, *et al.*: Contrast and stability of the axon diameter index from microstructure imaging with diffusion MRI. *Magn Reson Med*. 2013; 70(3): 711–21.  
[PubMed Abstract](#) | [Publisher Full Text](#) | [Free Full Text](#)
63. Zhang H, Hubbard PL, Parker GJ, *et al.*: Axon diameter mapping in the presence of orientation dispersion with diffusion MRI. *NeuroImage*. 2011; 56(3): 1301–15.  
[PubMed Abstract](#) | [Publisher Full Text](#)
64. Drobnyak I, Zhang H, Ianuş A, *et al.*: PGSE, OGSE, and sensitivity to axon diameter in diffusion MRI: Insight from a simulation study. *Magn Reson Med*. 2016; 75(2): 688–700.  
[PubMed Abstract](#) | [Publisher Full Text](#) | [Free Full Text](#)
65. F Nilsson M, Lasić S, Drobnyak I, *et al.*: Resolution limit of cylinder diameter estimation by diffusion MRI: The impact of gradient waveform and orientation dispersion. *NMR Biomed*. 2017; 30(7): e3711.  
[PubMed Abstract](#) | [Publisher Full Text](#) | [Free Full Text](#) | [F1000 Recommendation](#)
66. Zhang H, Schneider T, Wheeler-Kingshott CA, *et al.*: NODDI: Practical *in vivo* neurite orientation dispersion and density imaging of the human brain. *NeuroImage*. 2012; 61(4): 1000–16.  
[PubMed Abstract](#) | [Publisher Full Text](#)
67. Batalle D, Hughes EJ, Zhang H, *et al.*: Early development of structural networks and the impact of prematurity on brain connectivity. *NeuroImage*. 2017; 149: 379–92.  
[PubMed Abstract](#) | [Publisher Full Text](#) | [Free Full Text](#)
68. Eaton-Rosen Z, Melbourne A, Orasanu E, *et al.*: Longitudinal measurement of the developing grey matter in preterm subjects using multi-modal MRI. *NeuroImage*. 2015; 111: 580–9.  
[PubMed Abstract](#) | [Publisher Full Text](#)
69. Kunz N, Zhang H, Vasung L, *et al.*: Assessing white matter microstructure of the newborn with multi-shell diffusion MRI and biophysical compartment models. *NeuroImage*. 2014; 96: 288–99.  
[PubMed Abstract](#) | [Publisher Full Text](#)
70. Scherrer B, Schwartzman A, Taquet M, *et al.*: Characterizing brain tissue by assessment of the distribution of anisotropic microstructural environments in diffusion-compartment imaging (DIAMOND). *Magn Reson Med*. 2016; 76(3): 963–77.  
[PubMed Abstract](#) | [Publisher Full Text](#) | [Free Full Text](#)
71. Eaton-Rosen Z, Scherrer B, Melbourne A, *et al.*: Investigating the maturation of microstructure and radial orientation in the preterm human cortex with diffusion MRI. *NeuroImage*. 2017; 162: 65–72.  
[PubMed Abstract](#) | [Publisher Full Text](#)
72. F Novikov DS, Kiselev VG, Jespersen SN: On modeling. *Magn Reson Med*. 2018; 79(6): 3172–93.  
[PubMed Abstract](#) | [Publisher Full Text](#) | [Free Full Text](#) | [F1000 Recommendation](#)
73. Grussu F, Schneider T, Tur C, *et al.*: Neurite dispersion: a new marker of multiple sclerosis spinal cord pathology? *Ann Clin Transl Neurol*. 2017; 4(9): 663–79.  
[PubMed Abstract](#) | [Publisher Full Text](#) | [Free Full Text](#)
74. Alexander DC: Maximum entropy spherical deconvolution for diffusion MRI. *Inf Process Med Imaging*. 2005; 19: 76–87.  
[PubMed Abstract](#) | [Publisher Full Text](#)
75. Anderson AW: Measurement of fiber orientation distributions using high angular resolution diffusion imaging. *Magn Reson Med*. 2005; 54(5): 1194–206.  
[PubMed Abstract](#) | [Publisher Full Text](#)
76. Dell'Acqua F, Rizzo G, Scifo P, *et al.*: A model-based deconvolution approach to solve fiber crossing in diffusion-weighted MR imaging. *IEEE Trans Biomed Eng*. 2007; 54(3): 462–72.  
[PubMed Abstract](#) | [Publisher Full Text](#)
77. Descoteaux M, Deriche R, Knösche TR, *et al.*: Deterministic and probabilistic tractography based on complex fibre orientation distributions. *IEEE Trans Med Imaging*. 2009; 28(2): 269–86.  
[PubMed Abstract](#) | [Publisher Full Text](#)
78. Tournier JD, Calamante F, Gadian DG, *et al.*: Direct estimation of the fiber orientation density function from diffusion-weighted MRI data using spherical deconvolution. *NeuroImage*. 2004; 23(3): 1176–85.  
[PubMed Abstract](#) | [Publisher Full Text](#)
79. Tuch DS, Reese TG, Wiegell MR, *et al.*: High angular resolution diffusion imaging reveals intravoxel white matter fiber heterogeneity. *Magn Reson Med*. 2002; 48(4): 577–82.  
[PubMed Abstract](#) | [Publisher Full Text](#)
80. Jeurissen B, Tournier JD, Dhollander T, *et al.*: Multi-tissue constrained spherical deconvolution for improved analysis of multi-shell diffusion MRI data. *NeuroImage*. 2014; 103: 411–26.  
[PubMed Abstract](#) | [Publisher Full Text](#)
81. Pieterman K, Batalle D, Dudink J, *et al.*: Cerebello-cerebral connectivity in the developing brain. *Brain Struct Funct*. 2017; 222(4): 1625–34.  
[PubMed Abstract](#) | [Publisher Full Text](#) | [Free Full Text](#)
82. Salvan P, Tournier JD, Batalle D, *et al.*: Language ability in preterm children is associated with arcuate fasciculi microstructure at term. *Hum Brain Mapp*. 2017; 38(8): 3836–47.  
[PubMed Abstract](#) | [Publisher Full Text](#) | [Free Full Text](#)
83. Raffelt D, Tournier JD, Rose S, *et al.*: Apparent Fibre Density: a novel measure for the analysis of diffusion-weighted magnetic resonance images. *NeuroImage*. 2012; 59(4): 3976–94.  
[PubMed Abstract](#) | [Publisher Full Text](#)
84. F Raffelt DA, Tournier JD, Smith RE, *et al.*: Investigating white matter fibre density and morphology using fixel-based analysis. *NeuroImage*. 2017; 144(Pt A): 58–73.  
[PubMed Abstract](#) | [Publisher Full Text](#) | [Free Full Text](#) | [F1000 Recommendation](#)
85. Ashburner J, Friston KJ: Voxel-based morphometry—the methods. *NeuroImage*.

- 2000; **11**(6 Pt 1): 805–21.  
[PubMed Abstract](#) | [Publisher Full Text](#)
86. Gaser C, Nenadic I, Buchsbaum BR, *et al.*: **Deformation-based morphometry and its relation to conventional volumetry of brain lateral ventricles in MRI.** *NeuroImage*. 2001; **13**(6 Pt 1): 1140–5.  
[PubMed Abstract](#) | [Publisher Full Text](#)
87. Leow AD, Klunder AD, Jack CR Jr, *et al.*: **Longitudinal stability of MRI for mapping brain change using tensor-based morphometry.** *NeuroImage*. 2006; **31**(2): 627–40.  
[PubMed Abstract](#) | [Publisher Full Text](#) | [Free Full Text](#)
88. Raffelt D, Tournier JD, Crozier S, *et al.*: **Reorientation of fiber orientation distributions using apodized point spread functions.** *Magn Reson Med*. 2012; **67**(3): 844–55.  
[PubMed Abstract](#) | [Publisher Full Text](#)
89. **F** Pannek K, Fripp J, George JM, *et al.*: **Fixel-based analysis reveals alterations in brain microstructure and macrostructure of preterm-born infants at term equivalent age.** *NeuroImage Clin*. 2018; **18**: 51–9.  
[PubMed Abstract](#) | [Publisher Full Text](#) | [Free Full Text](#) | [F1000 Recommendation](#)
90. Pecheva D, Tournier JD, Pietsch M *et al.*: **Fixel based analysis of white matter fibre density and morphology in the preterm brain.** *Proceedings of the International Society for Magnetic Resonance in Medicine*. 2018; 0843.  
[Reference Source](#)

# Open Peer Review

Current Referee Status:



---

## Editorial Note on the Review Process

F1000 Faculty Reviews are commissioned from members of the prestigious F1000 Faculty and are edited as a service to readers. In order to make these reviews as comprehensive and accessible as possible, the referees provide input before publication and only the final, revised version is published. The referees who approved the final version are listed with their names and affiliations but without their reports on earlier versions (any comments will already have been addressed in the published version).

---

## The referees who approved this article are:

### Version 1

- 1 **Hao Huang Qinlin Yu** Department of Radiology, Perelman School of Medicine, University of Pennsylvania, Pennsylvania, USA  
**Competing Interests:** No competing interests were disclosed.
- 2 **Risto A Kauppinen** School of Experimental Psychology and Clinical Research and Imaging Centre, University of Bristol, Bristol, UK  
**Competing Interests:** No competing interests were disclosed.

The benefits of publishing with F1000Research:

- Your article is published within days, with no editorial bias
- You can publish traditional articles, null/negative results, case reports, data notes and more
- The peer review process is transparent and collaborative
- Your article is indexed in PubMed after passing peer review
- Dedicated customer support at every stage

For pre-submission enquiries, contact [research@f1000.com](mailto:research@f1000.com)

F1000Research